Microenvironment and Immunology

Cancer Research

Lung Metastasis Fails in MMTV-PyMT Oncomice Lacking S100A4 Due to a T-Cell Deficiency in Primary Tumors

Birgitte Grum-Schwensen[1], Jörg Klingelhöfer[1], Mariam Grigorian[1], Kasper Almholt[2], Boye Schnack Nielsen[2], Eugene Lukanidin[1], and Noona Ambartsumian[1]

Abstract

Interactions between tumor and stroma cells are essential for the progression of cancer from its initial growth at a primary site to its metastasis to distant organs. The metastasis-stimulating protein S100A4 exerts its function as a stroma cell–derived factor. Genetic depletion of S100A4 significantly reduced the metastatic burden in lungs of PyMT-induced mammary tumors. In S100A4$^{+/+}$ PyMT mice, massive leukocyte infiltration at the site of the growing tumor at the stage of malignant transition was associated with increased concentration of extracellular S100A4 in the tumor microenvironment. In contrast, in S100A4$^{-/-}$ PyMT tumors, a significant suppression of T-cell infiltration was documented at the transition period. *In vitro*, the S100A4 protein mediated the attraction of T cells. Moreover, S100A4$^{+/+}$, but not S100A4$^{-/-}$, fibroblasts stimulated the invasion of T lymphocytes into fibroblast monolayers. *In vivo*, the presence of S100A4$^{+/+}$, but not S100A4$^{-/-}$, fibroblasts significantly stimulated the attraction of T lymphocytes to the site of the growing tumor. Increased levels of T cells were also observed in the premetastatic lungs of tumor-bearing mice primed to metastasize by S100A4$^{+/+}$ fibroblasts. Treatment of T cells with the S100A4 protein stimulated production of cytokines, particularly granulocyte colony-stimulating factor and eotaxin-2. The same cytokines were detected in the fluid of S100A4$^{+/+}$ PyMT tumors at the transition period. We suggest that release of S100A4 in the primary tumor stimulates infiltration of T cells and activates secretion of cytokines, thus triggering sequential events that fuel tumor cells to metastasize. Similar processes could occur in the premetastatic lungs, facilitating generation of inflammatory milieu favorable for metastasis formation. *Cancer Res; 70(3); 936–47. ©2010 AACR.*

Introduction

An accumulating body of evidence indicates that responses of stroma cells in neoplastic tissues stimulate tumor progression and subsequent metastatic spread. These cells include fibroblasts, vascular cells, infiltrating leukocytes, as well as bone marrow–derived myeloid cells (1). Leukocytes from both lineages, myeloid and lymphoid, have been shown to regulate cancer development. The mechanisms underlying the response of immune cells to a particular tumor are poorly understood. For example, macrophages are capable of modifying cancer cell behavior and promoting tumor invasion and metastasis. Contra wise, they can show pronounced antitumorigenic activity (2, 3).

Authors' Affiliations: [1]Department of Molecular Cancer Biology, Danish Cancer Society; [2]Finsen Laboratory, Rigshospitalet, Copenhagen, Denmark

Note: Supplementary data for this article are available at Cancer Research Online (http://cancerres.aacrjournals.org/).

Current address for K. Almholt: Histology, Novo Nordisk A/S, Novo Nordisk Park, Måløv, Denmark. Current address for B.S. Nielsen: Exiqon A/S, Vedbaek, Denmark.

Corresponding Author: Noona Ambartsumian, Department of Molecular Cancer Biology, Danish Cancer Society, Strandboulevarden 49, DK-2100 Copenhagen, Denmark. Phone: 45-3525-7356; Fax: 45-3525-7721; E-mail: na@cancer.dk.

doi: 10.1158/0008-5472.CAN-09-3220

©2010 American Association for Cancer Research.

The roles of tumor-infiltrating lymphocytes, B cells, and various proportions of CD4$^+$ and CD8$^+$ T cells in metastatic progression are much less understood (4).

The presence of CD8$^+$ CTLs normally reflects a strong antitumor response. In contrast, CD4$^+$ T-helper cells play a tumor-promoting role. It has been shown that Th2-polarized T-helper cells downregulate cell-mediated antitumor immunity and enhance protumor immune responses (4). Among CD4$^+$ cells, a subset of regulatory T cells is increased in tumors and is capable of suppressing proliferation of other T cells in the microenvironment (5). Recent data strongly linked CD4$^+$ T cells with stimulation of metastasis (6). T cells secrete growth factors and cytokines, which support tumor angiogenesis and recruit macrophages, thus accelerating tumor growth and metastasis (1).

The transgenic mouse model based on the expression of polyoma virus middle T oncoprotein placed under control of mouse mammary tumor virus promoter, thereby directing expression of the oncogene to the mammary gland (MMTV-PyMT mice), is widely used to study the effect of different genes on mammary tumorigenesis (7). In MMTV-PyMT mice, four distinctly identifiable stages of tumor progression from premalignant to malignant are described in detail, making this model a useful tool for studying tumor progression (8).

S100A4, a member of the S100 family of calcium-binding proteins, promotes tumor metastasis (9). Poor prognostic outcomes of a variety of human cancers were correlated

Downloaded from http://aacrjournals.org/cancerres/article-pdf/70/3/936/2644381/936.pdf by guest on 13 April 2024

with S100A4 expression (10). Accumulating lines of evidence indicate that S100A4 stimulates metastasis as an extracellular factor. Indeed, S100A4 is predominantly expressed and released from breast cancer stroma cells (11). Its secretion can be stimulated *in vitro* from fibroblasts and other cells that compose the tumor stroma (12). As an extracellular protein, S100A4 acts as an angiogenic factor; stimulates neurite outgrowth, cell survival, and tumor cell migration; and activates epidermal growth factor receptor, the transcription factor NF-κB, and the mitogen-activated protein (MAP) kinase pathway, leading to the activation of downstream genes (13–19). Moreover, we found that tumor graft development and metastasis formation is impeded in mice deficient in S100A4 (20). Recent data implicate extracellular S100A4 in various inflammation-associated noncancer pathologies (21).

In the present study, we implemented the MMTV-PyMT tumor model to study the influence of S100A4 expression at early stages of tumor development on metastasis formation. We present lines of evidence that S100A4 released into the tumor microenvironment at a stage of malignant transition from adenoma/MIN to early carcinoma induces massive infiltration of T cells and release of specific cytokines, leading to increased pulmonary metastases. Infiltration of T cells in premetastatic lungs was induced by $S100A4^{+/+}$ fibroblasts, probably generating a favorable microenvironment for metastasis formation.

Materials and Methods

Reagents. S100A4 protein was isolated as described by Novitskaya and colleagues (14). SDF-1α was purchased from PeproTech, and fibronectin was from Sigma-Aldrich. RPMI 1640, Opti-MEM, and FCS were purchased from Invitrogen.

Mice. Virgin females of $S100A4^{+/+}$ PyMT and $S100A4^{-/-}$ PyMT genotype or $S100A4^{-/-}$ mice of A/Sn genetic background were used for experiments. See details of breeding and genotyping in Supplementary Data. All animals were maintained according to the Federation of European Laboratory Animal Science Associations guidelines for the care and use of laboratory animals.

Metastasis assay. CSML100 mouse mammary carcinoma cells (1×10^6) expressing enhanced green fluorescent protein (EGFP) were injected s.c. to $S100A4^{-/-}$ A/Sn mice followed by i.v. injection of 2.5×10^5 $S100A4^{+/+}$ or $S100A4^{-/-}$ mouse embryonic fibroblasts (MEF; ref. 20).

Injections of MEFs were repeated three times with 1-wk intervals. Animals were either sacrificed 1 wk after the last injection (premetastatic phase) or left until the tumor reached maximum allowed size (864 mm^3; metastatic phase). Lungs were isolated and subjected to standard immunohistochemical analysis.

Immunohistochemistry. Tumor tissue sections were stained with affinity-purified rabbit polyclonal antibodies against S100A4 (22), anti-CD3 (Abcam), anti-F4/80 (Accurate Chemicals), anti–α-smooth muscle actin and anti-laminin (Sigma-Aldrich), anti-CD31 and anti-CD45 (BD Biosciences), and anti-EGFP (Santa Cruz Biotechnology) according to the manufacturer's protocols. Corresponding secondary horseradish peroxidase–conjugated antibodies were used followed by incubation with chromogenic substrate 3,3′-diaminobenzidine (DAKO). For double staining, secondary antibodies coupled to Alexa Fluor 488 or Alexa Fluor 568 (1:1,500) were purchased from Molecular Probes. Sections were examined by means of confocal microscopy on a LSM 510 (Carl Zeiss, Inc.). The blood vessel density was determined by quantifying the amount of $CD31^+$ capillaries in 10 fields from two sections of different parts of the tumor (magnification, ×200). $S100A4^+$ cells, leukocytes, macrophages, and T lymphocytes were quantified by determining the amount of $S100A4^+$, $CD45^+$, $F4/80^+$, and $CD3^+$ cells in 10 fields from two sections of different parts of the PyMT tumors (magnification, ×400) obtained from mice ages 6 (n = 5), 8 (n = 4), 12 (n = 5), and 18 ± 5 (n = 10) wk. Quantification of T cells in tumor xenografts was performed using paraffin blocks from the study (n = 10 per group; ref. 20).

Quantification of leukocytes and T cells in the vicinity of blood vessels in premetastatic lungs was performed by counting fluorescently labeled $CD45^+$ (n = 10–15 mice per group) and $CD3^+$ cells (n = 10–12 per group) in the surrounding of vessels visualized by staining with anti–smooth muscle actin antibodies. Ten vessels of 100 to 200 nm in length per section were selected for analysis.

Sandwich ELISA assays. S100A4 sandwich ELISA was used to determine the amount of S100A4 in the mouse tumor interstitial fluids (TIF). For TIF analysis, 50 mg of tumor tissue were removed and incubated for 2 h at 37°C in 1,000 μL PBS as described by Celis and colleagues (23).

Sandwich ELISA was done as described (13). A granulocyte colony-stimulating factor (G-CSF) ELISA kit (RayBiotech) was used to determine G-CSF concentration in cell culture–conditioned medium and TIFs according to the manufacturer's instructions.

T-lymphocyte purification by magnetic cell sorting. Spleens were removed from mice, and single-cell suspensions were layered onto Histopaque (Sigma-Aldrich) and centrifuged to remove RBCs. Cells were purified by negative selection using the Pan T Cell Isolation kit (Miltenyi Biotech) according to the manufacturer's instructions. The purity of the T lymphocyte fraction assessed by flow cytometry analysis was >90%. Cells were cultured in RPMI 1640 with 10% FCS.

Chemotaxis assay. *In vitro* chemotaxis assay with Transwell chambers (pore size, 5 μm) obtained from Corning was conducted as described (24). Transwells were coated with 50 μg/mL fibronectin at 4°C overnight. A total of 1×10^6 purified T cells in 100 μL RPMI 1640 with 1% FCS were added to the upper chamber. The S100A4 protein was added either alone or together with rabbit Ig (DAKO) or anti-S100A4 antibodies to the bottom chamber (22). SDF-1α (100 ng/mL) was used as a positive control in each experiment. After 90 min at 37°C, migrated cells were collected and counted. The experiments were performed in duplicate and repeated a minimum of three times.

T-lymphocyte invasion assay. Invasion of T lymphocytes into fibroblast monolayers was tested using a modification

Downloaded from http://aacrjournals.org/cancerres/article-pdf/70/3/936/2644381/936.pdf by guest on 13 April 2024

of the method (25). MEFs were grown to confluency in 24-well plates; T lymphocytes were labeled with Vybrant DID cell-labeling solution (Invitrogen) according to the manufacturer's instructions. Labeled T lymphocytes (7×10^5) were added to the wells and incubated for 4 h. Noninvaded cells were removed by washing and mechanical agitation four times in PBS. The infiltrated cells were counted using a fluorescence microscope (Zeiss, Metamorph software) in three random fields (magnification, ×100) per well. Invasion assays were performed in RPMI 1640 containing 10% FCS with or without rabbit Ig (DAKO) or anti-S100A4 antibodies. The experiments were performed in triplicates and repeated twice.

Cytokine antibody array and Western blot analyses. Purified T lymphocytes (1×10^7) were treated with the multimeric S100A4 (1 μg/mL) for 19 h in Opti-MEM supplemented with 10 μg/mL polymyxin B (Invitrogen). The conditioned medium was harvested and filtered through a 0.45-μm membrane. Cell viability was checked using LDH Cytotoxicity Detection kit (Roche) according to the manufacturer's protocol.

TIFs from 12-wk-old S100A4$^{+/+}$ PyMT (n = 5) and 12-wk-old S100A4$^{-/-}$ PyMT mouse tumors (n = 5) were pooled. The protein concentrations in TIFs were measured and equilibrated.

RayBio Mouse Cytokine Antibody Arrays 3 and 4 were purchased from RayBiotech, and the cytokine analyses in conditioned medium and TIFs were carried out according to the manufacturer's instructions.

Purified T cells were starved in RPMI 1640 for 3 h and stimulated with multimeric S100A4 (1 μg/mL) or with SDF-1α (100 ng/mL). Cell lysates were prepared in the presence of phosphatase inhibitors and resolved by SDS-PAGE. Activation of MAP kinase pathway was analyzed using a standard Western blot procedure with phospho-p44/42 extracellular signal-regulated kinase 1/2 (ERK1/2; Thr^{202}/Tyr^{204}) and p44/42 ERK1/2 antibodies (Cell Signaling Technology).

Statistical analyses. Data are presented as average ± SEM. The confidence level was calculated using Student's t test.

Results

S100A4 deficiency suppresses metastases of mammary tumors of MMTV-PyMT mice. To investigate the role of S100A4 at early stages of metastatic breast cancer development, we induced mammary carcinogenesis in wild-type and S100A4$^{-/-}$ mice by using the MMTV-PyMT transgenic model. Comparison of the tumor development showed similar growth pattern both in the S100A4$^{-/-}$ and in the S100A4$^{+/+}$ PyMT mice (Supplementary Table S1).

Analysis of the lung sections from 18 ± 5-week-old tumor-bearing animals showed that the number of metastatic nodules and the overall metastatic burden were both significantly suppressed in S100A4$^{-/-}$ PyMT mice (Fig. 1A and B).

The grading of tumors showed that tumors developed in mice at the age of 12 weeks represented a period of transition to malignancy (Supplementary Table S2). Because we aimed to study early stages of tumor development, 12-week-old mice were used for further analysis.

Decreased metastatic burden in lungs of S100A4$^{-/-}$ PyMT mice is associated with reduced vessel density. Because the S100A4 protein is an angiogenic factor (13, 17) we proposed that suppression of lung metastases in S100A4$^{-/-}$ PyMT mice might be associated with the suppression of angiogenesis in the primary tumor. Consequently, we compared the vascular density of the primary tumors of the 18 ± 5-week-old tumor-bearing S100A4$^{-/-}$ and S100A4$^{+/+}$ PyMT mice. To assure accurate verification of vessel density, we determined the number of capillaries in morphologically different histopathologic compartments of the section (Fig. 1C). In compartments corresponding to both early and late carcinoma, the vessel density in the S100A4$^{+/+}$ tumors was significantly higher when compared with S100A4$^{-/-}$ tumors (Fig. 1C). The same tendency was observed in the adenoma/MIN compartment, although the difference was not statistically significant.

S100A4 is released at early stage of PyMT mammary tumor development. To associate increased vessel density with S100A4 expression, we performed immunohistochemical staining of tumor sections from S100A4$^{+/+}$ PyMT mice at different ages with anti-S100A4 antibodies (Fig. 2A). As expected, independently of the stage of tumor development, S100A4 was expressed mostly in tumor stroma. S100A4$^+$ stroma cells were found most abundant in sections displaying adenoma/MIN and early carcinoma, which corresponded to the transition from premalignant lesion to malignant tumor (8), whereas late carcinoma contained far fewer S100A4$^+$ stroma cells. Interestingly, pulmonary metastases also contained S100A4$^+$ cells accumulated in the area of the lesion (data not shown). Quantification of the number of S100A4$^+$ cells localized in different compartments of the tumor showed that the majority of S100A4$^+$ cells were concentrated in the area surrounding adenoma/MIN–early carcinoma (Fig. 2B).

Further, we correlated the release of S100A4 into the tumor microenvironment with the accumulation of S100A4$^+$ stroma cells.

Examination of the S100A4 protein concentrations in TIFs from tumors isolated from 6-, 8-, 12-, and 18 ± 5-week-old mice revealed substantial increase of S100A4 in TIFs from 12-week-old mice containing adenoma/MIN–early carcinoma compared with TIFs from 6- to 8-week-old mice containing mostly normal mammary gland and hyperplasia (Fig. 2*C*). The concentration of S100A4 in late carcinomas was reduced (Fig. 2C). Fluctuation of extracellular S100A4 concentration showed a good correlation with the abundance of S100A4$^+$ cells in stroma of tumors at distinct stages of development (Fig. 2B).

Decreased infiltration of T cells in S100A4$^{-/-}$ tumors. Based on our studies of tumor growth in S100A4$^{-/-}$ mice (20), we expected a decrease in leukocyte infiltration in tumors of S100A4$^{-/-}$ PyMT mice. Indeed, we revealed a remarkable shortage of CD45$^+$ leukocytes infiltrating S100A4$^{-/-}$ PyMT tumors (Fig. 3A). Quantification of the number of leukocytes surrounding different histopathologic compartments of the tumor showed a significant decrease in the area of adenoma/MIN in S100A4$^{-/-}$ compared with

Downloaded from http://aacrjournals.org/cancerres/article-pdf/70/3/936/2644381/936.pdf by guest on 13 April 2024

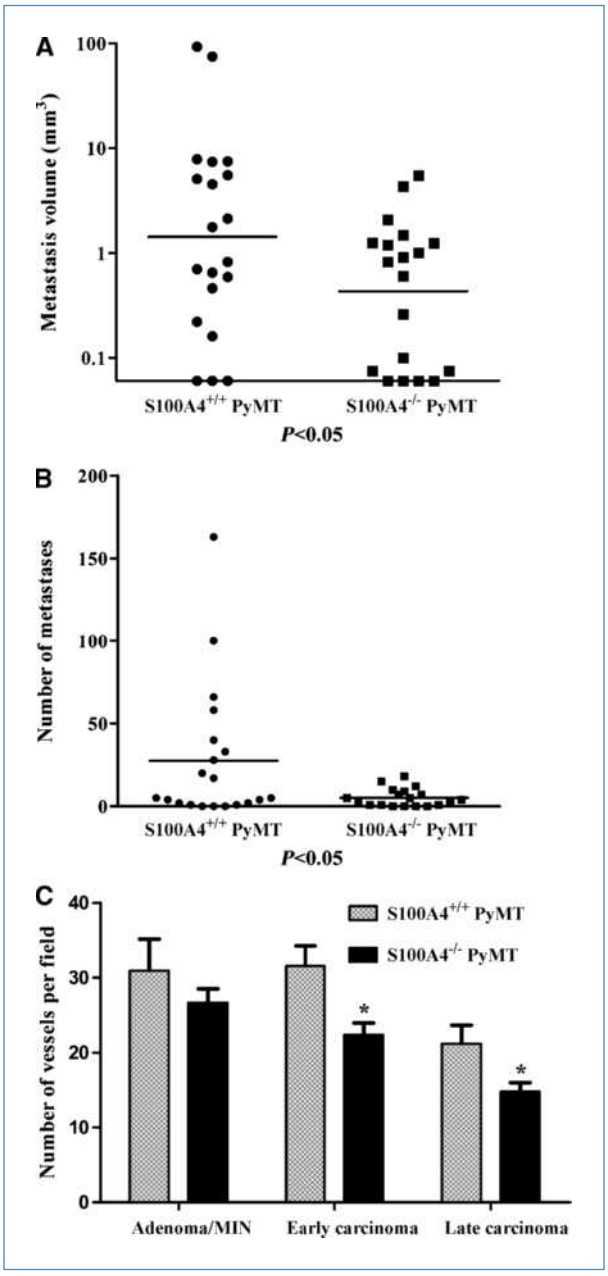

Figure 1. Lung metastases development and vessel density of primary S100A4$^{-/-}$ and S100A4$^{+/+}$ PyMT tumors. A, lung metastases volume in S100A4$^{+/+}$ PyMT (n = 20) and S100A4$^{-/-}$ PyMT (n = 19) mice. B, number of metastatic foci per lung per mouse in S100A4$^{+/+}$ PyMT and S100A4$^{-/-}$ PyMT mice. C, vessel density of primary tumors developed in S100A4$^{+/+}$ PyMT (n = 10) and S100A4$^{-/-}$ PyMT (n = 10) mice. *, $P < 0.05$.

S100A4$^{+/+}$ PyMT tumors (Fig. 3B). Lin and colleagues (2) recently showed an increase in macrophage infiltration in premalignant tumors of wild-type PyMT mice that play a causal role in regulating the angiogenic switch and progression to malignancy. We therefore assessed the amount of macrophages infiltrating early developing tumors in S100A4$^{+/+}$ and S100A4$^{-/-}$ PyMT mice. Indeed, macrophages heavily infiltrated the vicinity of adenoma/MIN but not hyperplasia in both 8- and 12-week-old mice (Fig. 3C). Quantification of the infiltrating macrophages showed a tendency toward lower abundance in S100A4$^{-/-}$ tumors of 8-week-old mice; however, the difference was not statistically significant (P = 0.11).

In contrast to macrophages, comparison of the numbers of infiltrating T lymphocytes at different stages of tumor development revealed that S100A4 deficiency led to substantially reduced numbers of T cells infiltrating adenoma/MIN (Fig. 3D).

S100A4 attracted T lymphocytes* in vitro *and activated the MAP kinase pathway. Our observations thus far suggested that S100A4 could be a mediator of T lymphocyte infiltration into the tumor. We therefore tested the attraction of T cells isolated from spleens of S100A4$^{+/+}$ and S100A4$^{-/-}$ mice toward S100A4 in a Transwell migration assay. These experiments showed that S100A4 was capable to attract T lymphocytes from both sources in a concentration-dependent manner. Moreover, S100A4 antibodies blocked S100A4-induced chemoattraction of T cells (Fig. 4A). The ratio between nonmigrated and migrated CD4$^+$/CD8$^+$ and CD4$^+$/CD25$^+$ T-cell populations was determined by flow cytometry and did not reveal any differences between S100A4$^{+/+}$ and S100A4$^{-/-}$ splenocytes (data not shown).

We also tested the capability of naturally produced S100A4 to attract T lymphocytes. It has been shown that MEFs stimulate tumor progression and release S100A4 into the cell culture medium *in vitro* (12, 20). T-cell monolayer invasion assays (26) showed that T lymphocytes failed to invade into S100A4$^{-/-}$ MEF monolayer, whereas S100A4$^{+/+}$ MEFs strongly attracted T lymphocytes. Moreover, S100A4 antibodies blocked T lymphocyte invasion into the S100A4$^{+/+}$ MEF monolayer (Fig. 4B).

It is known that cells respond to S100A4 treatment via activation of the MAP kinase pathway (14).

Therefore, we tested whether the ERK1/2 signal-regulated kinases are phosphorylated in T cells in response to S100A4 treatment. Figure 4C shows the time-dependent activation of S100A4-induced phosphorylation of ERK1/2, whereas S100A4 had no effect on p38 kinase phosphorylation (data not shown).

S100A4$^{+/+}$ MEFs stimulate attraction of T lymphocytes to the tumor grafts. Suppression of tumor development and metastasis formation due to the aberrant stroma formation was earlier observed in S100A4$^{-/-}$ mice. Addition of S100A4$^{+/+}$ MEFs to the xenografts resulted in stimulation of tumor development associated with the increase of S100A4 in TIFs (20). Therefore, we proposed that tumor growth stimulation by S100A4$^{+/+}$ MEFs is associated with the attraction of T cells to the tumor stroma.

Indeed, tumor grafts supplied with S100A4$^{+/+}$ in contrast to S100A4$^{-/-}$ MEFs attracted more T cells to the stroma (Fig. 4D).

S100A4$^{+/+}$ MEFs facilitate attraction of T cells to the pre-metastatic lungs. As it was mentioned above, we observed accumulation of S100A4$^+$ cells at the site of metastases in lungs of tumor-bearing PyMT mice. We therefore proposed

Downloaded from http://aacrjournals.org/cancerres/article-pdf/70/3/936/2644381/936.pdf by guest on 13 April 2024

that the attraction of T cells could be associated with the formation of secondary tumors in the lungs. To assess the role of T cells in metastasis formation, we generated a model where metastatic mammary carcinoma cells, CSML100, whose metastatic ability was suppressed in S100A4$^{-/-}$ mice (20), were primed to metastasize by supplying animals with S100A4$^{+/+}$ MEFs by i.v. administration (see Materials and Methods for details). Analysis of the pulmonary metastases in the tumor-bearing mice in metastatic stage (maximal size of the tumor) showed that 28% (n = 7) of mice contained detectable metastatic nodules in the lungs. Lungs of tumor-bearing mice on premetastatic stage contained solitary tumor cells with a scattered distribution within the lungs. The identity of tumor cells was determined by immunostaining of consecutive sections with S100A4 (Fig. 5A) and EGFP antibodies (Supplementary Fig. S1). Administration of S100A4$^{+/+}$ MEFs significantly increased the amount of tumor cells present in the lungs (Fig. 5A). Moreover, lungs of tumor-bearing mice with S100A4$^{+/+}$ MEF administration but not S100A4$^{-/-}$ MEFs showed pronounced accumulation of leukocytes in the vicinity of blood vessels. Monoinjection of S100A4$^{+/+}$ and S100A4$^{-/-}$ MEFs or CSML100 cells did not reveal leukocyte accumulation (Fig. 5B). Quantification of T cells showed significant increase in the amount of T cells accumulated around the vessels in the premetastatic lungs supplied with S100A4$^{+/+}$ MEFs (Fig. 5C). Obtained data indicate that T cells can participate in the preconditioning of secondary organs to accept tumor cells and develop metastasis.

S100A4 stimulates production of cytokines from T lymphocytes. The capability of S100A4 to activate T cells was tested by its ability to stimulate the cytokine production. Indeed, T lymphocytes stimulated by S100A4 produced increased levels of 11 cytokines and growth factors as

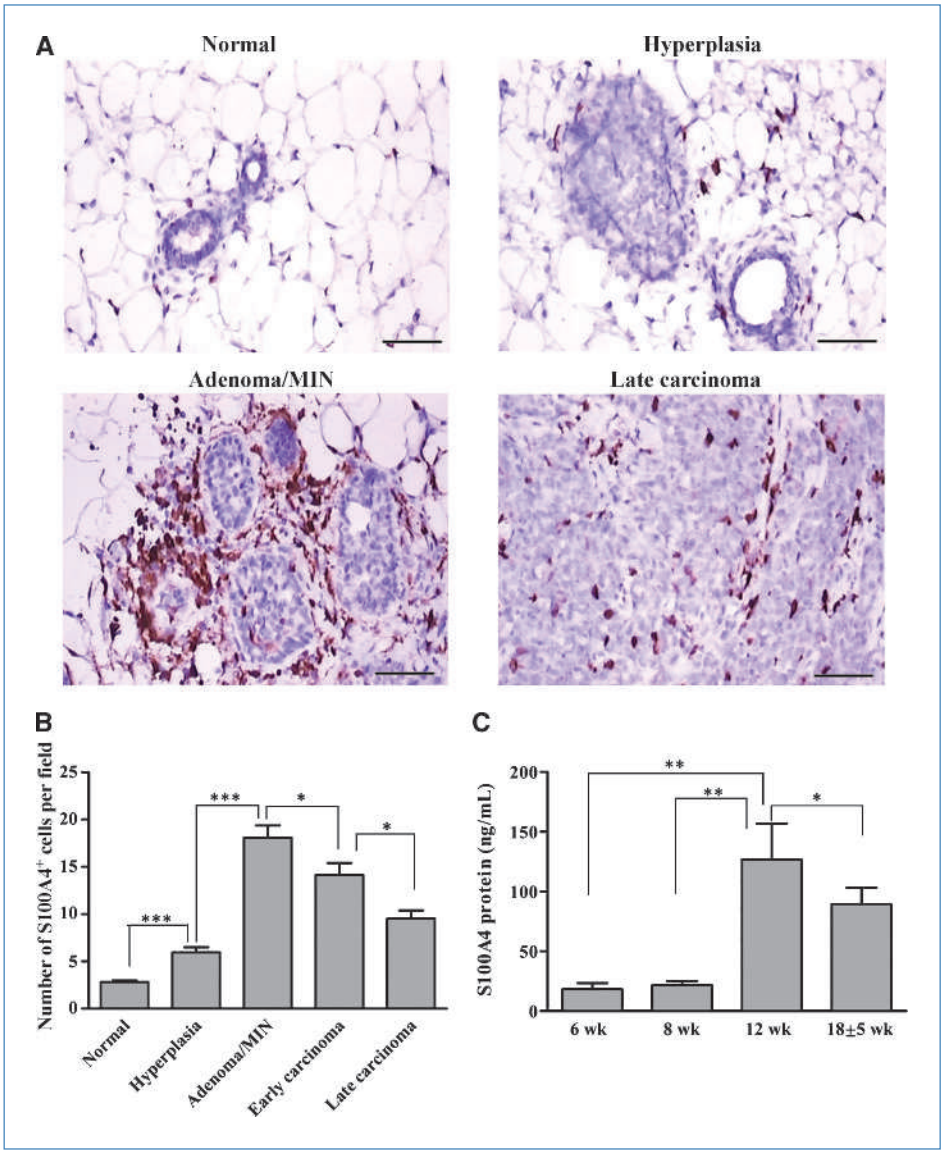

Figure 2. Expression and secretion of S100A4 protein from primary PyMT tumors. A, immunohistochemical analysis of S100A4 expression at different stages of tumor development (representative images are shown). S100A4$^+$ stroma cells are most abundant in the vicinity of adenoma/MIN and less abundant in late carcinoma. Scale bars, 50 μm. B, quantification of S100A4$^+$ cells surrounding normal mammary gland, hyperplasia, adenoma/MIN, and late carcinoma. C, concentration of the S100A4 protein in the TIFs from mice ages 6, 8, 12, and 18 ± 5 wk, respectively. *, $P < 0.05$; **, $P < 0.01$; ***, $P < 0.001$.

Downloaded from http://aacrjournals.org/cancerres/article-pdf/70/3/936/2644381/936.pdf by guest on 13 April 2024

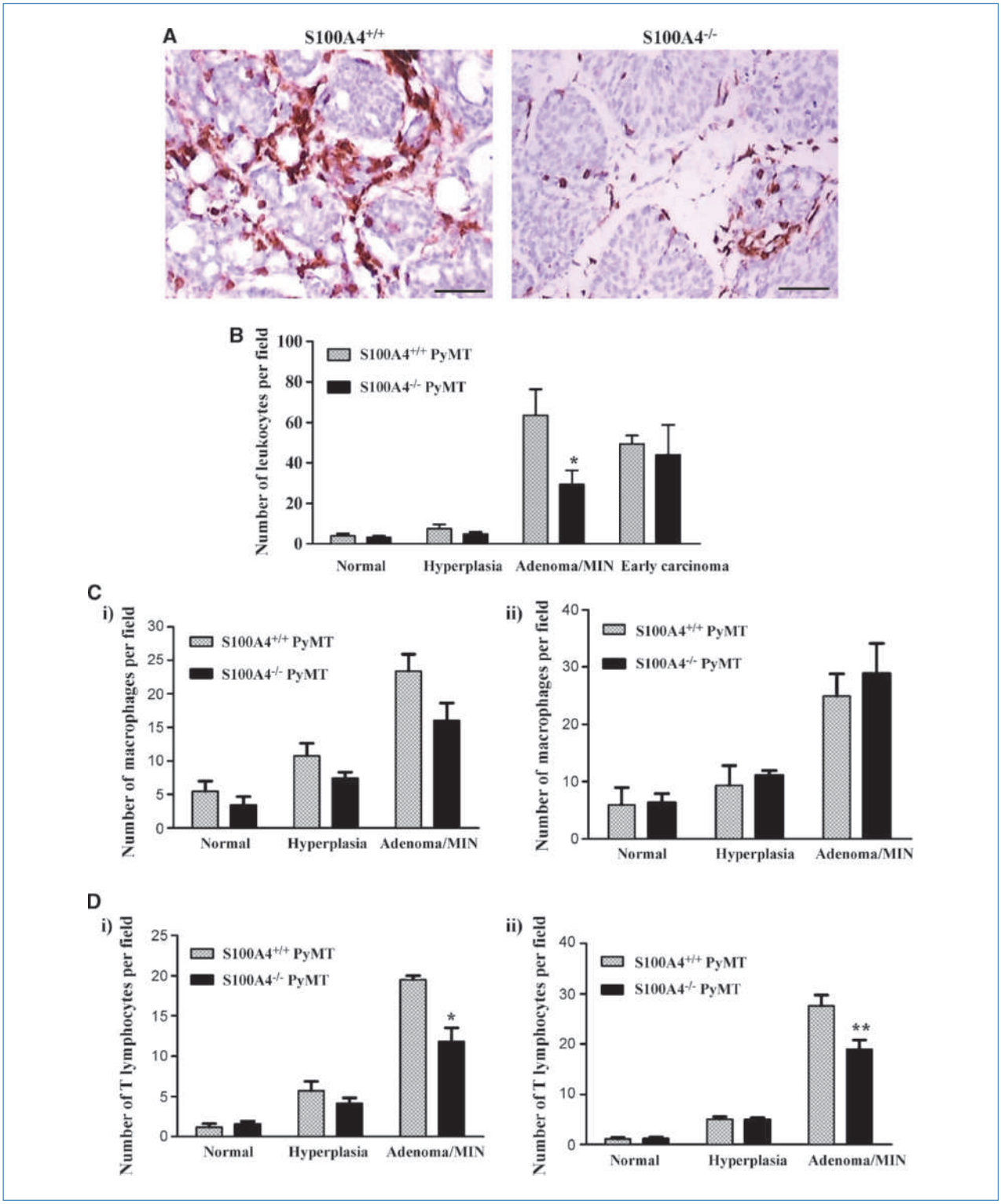

Figure 3. Accumulation of leukocytes in S100A4$^{-/-}$ and S100A4$^{+/+}$ PyMT tumors. A, CD45^{+} leukocytes in tumors from 12-wk-old PyMT mice with adenoma/MIN (representative images are shown). Scale bars, 50 μm. B, quantification of leukocytes surrounding normal mammary gland, hyperplastic, adenoma/MIN, and early carcinoma lesions of 12-wk-old S100A4$^{+/+}$ and S100A4$^{-/-}$ PyMT mice. C, quantification of F4/80^{+} macrophages surrounding normal mammary glands, hyperplastic, and adenoma/MIN lesions. D, quantitative evaluation of CD3^{+} T lymphocytes surrounding normal mammary glands, hyperplastic, and adenoma/MIN lesions. The numbers of T cells and macrophages were determined in S100A4$^{+/+}$ and S100A4$^{-/-}$ PyMT tumors from 8-wk-old (i) and 12-wk-old (ii) mice. *, $P < 0.05$; **, $P < 0.01$.

Downloaded from http://aacrjournals.org/cancerres/article-pdf/70/3/936/2644381/936.pdf by guest on 13 April 2024

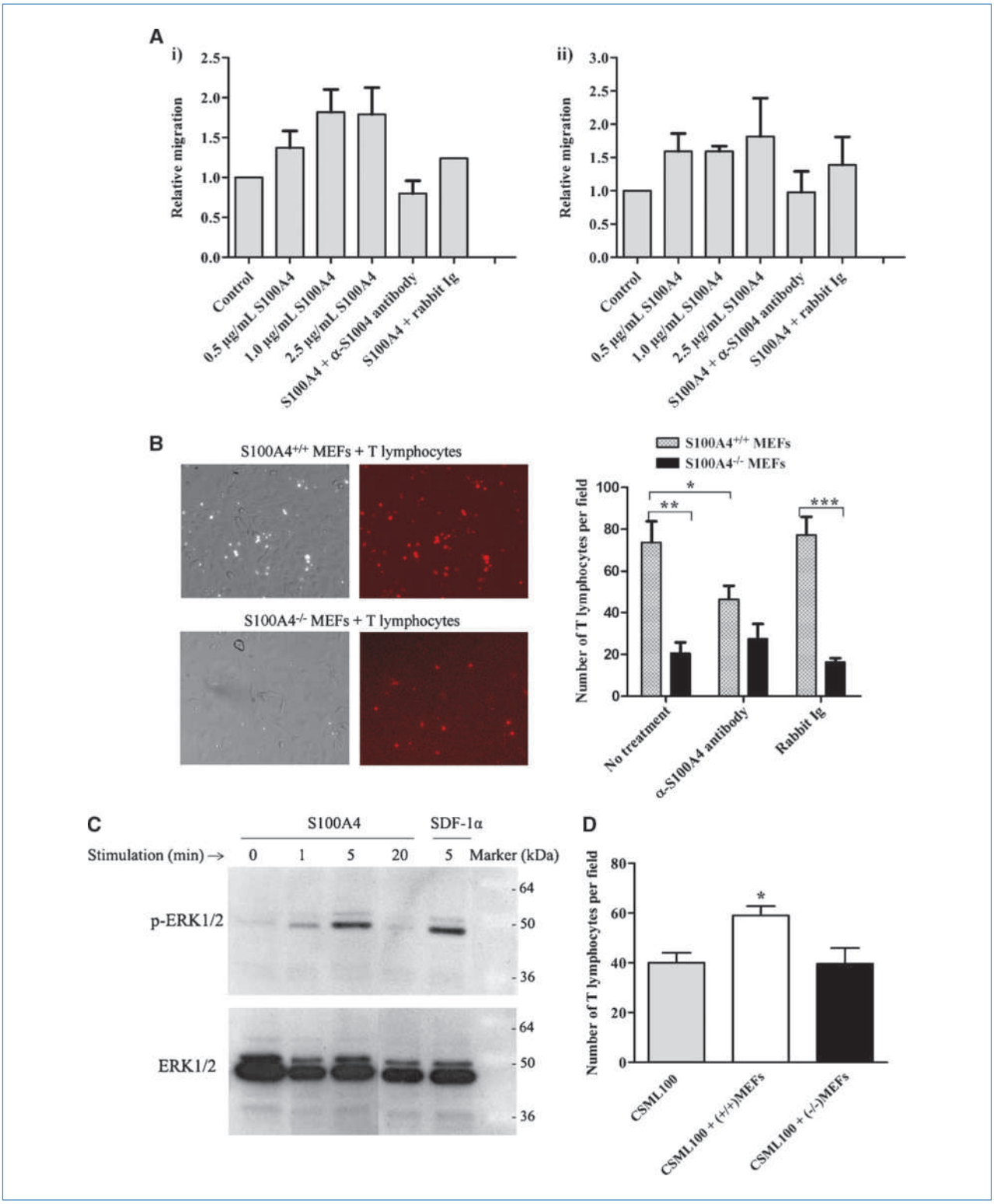

Figure 4. The S100A4 protein attracts T lymphocytes *in vitro* and *in vivo*. A, relative migration of T cells isolated from S100A4$^{+/+}$ (i) and S100A4$^{-/-}$ (ii) mice toward the S100A4 protein. S100A4 antibodies but not rabbit Ig block S100A4-induced chemoattraction of T lymphocytes. B, invasion of T lymphocytes (red) into monolayers of S100A4$^{+/+}$ and S100A4$^{-/-}$ MEFs. Invasion of T lymphocytes into the S100A4$^{+/+}$ monolayer was blocked by S100A4 antibodies. C, phosphorylation of ERK1/2 in response to S100A4 or SDF-1α stimulation of T lymphocytes at the indicated times. D, quantification of T lymphocytes in CSML100 tumor xenografts. CSML100 xenografts were injected to S100A4$^{-/-}$ mice alone or together with S100A4$^{+/+}$ or S100A4$^{-/-}$ MEFs. *, $P < 0.05$; **, $P < 0.01$; ***, $P < 0.001$.

Downloaded from http://aacrjournals.org/cancerres/article-pdf/70/3/936/2644381/936.pdf by guest on 13 April 2024

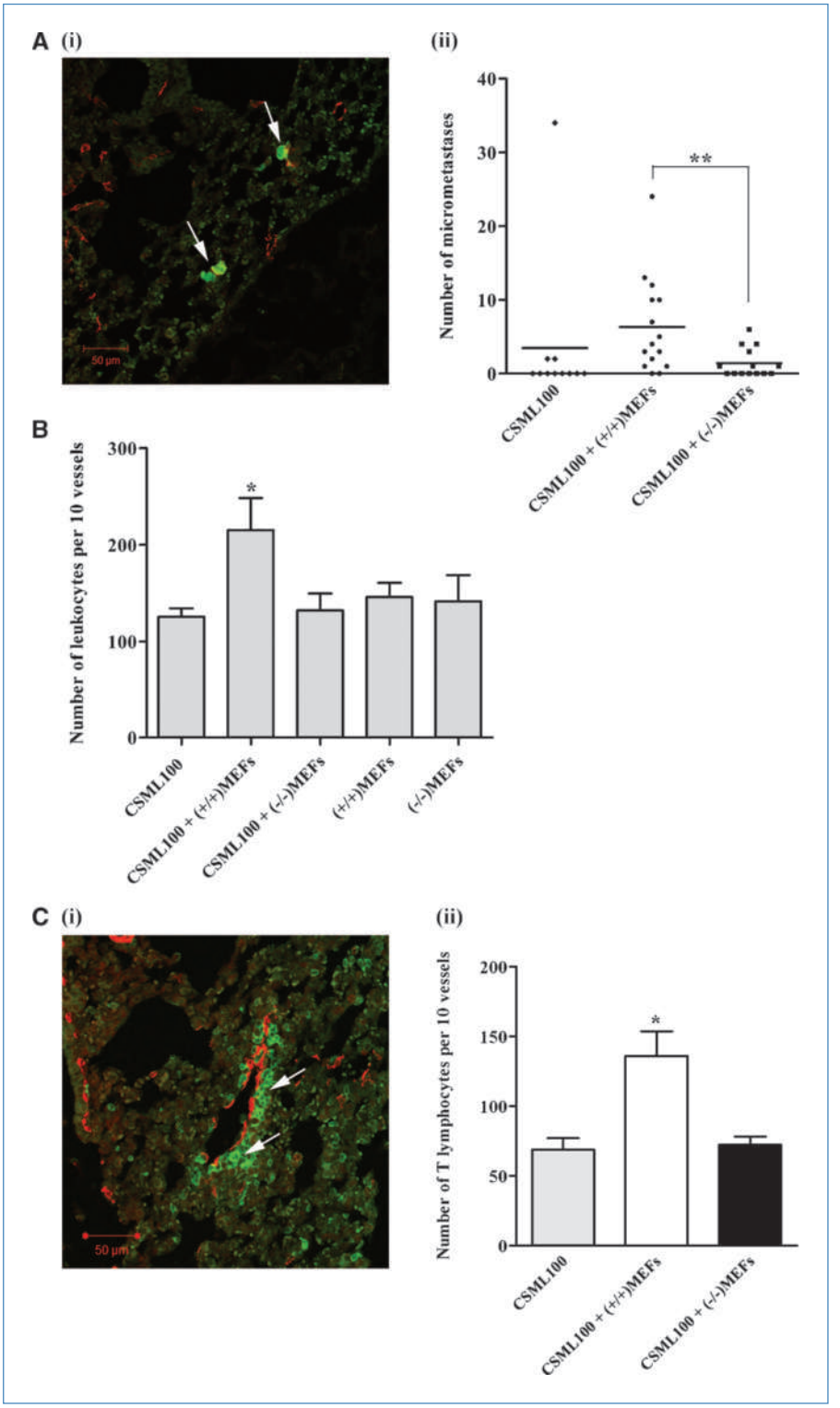

Figure 5. S100A4$^{+/+}$ MEFs facilitate attraction of T cells to the premetastatic lungs. A, i, S100A4^{+} tumor cells (green) in premetastatic lungs; ii, quantification of tumor cells in premetastatic lungs of mice grafted with CSML100 alone or supplied with S100A4$^{+/+}$ or S100A4$^{-/-}$ MEFs i.v. B, quantification of CD45^{+} leukocytes concentrated around vessels in lungs from mice grafted with CSML100 alone or supplied with S100A4$^{+/+}$ or S100A4$^{-/-}$ MEFs i.v. or injected alone with MEFs. C, i, CD3^{+} T cells (green) surrounding blood vessels (red) in lungs of tumor-bearing mice; ii, quantification of T cells surrounding vessels in lungs from mice transplanted with CSML100 alone or supplied with S100A4$^{+/+}$ or S100A4$^{-/-}$ MEFs i.v. *, $P < 0.05$; **, $P < 0.01$.

assessed by cytokine antibody array (Fig. 6A). Further, cytokine antibody array analysis of TIFs isolated from 12-week-old PyMT mice detected enhanced levels of seven cytokines in S100A4$^{+/+}$ PyMT compared with S100A4$^{-/-}$ TIFs (Fig. 6B). Levels of two cytokines, G-CSF and eotaxin-2 (CXCL-24), were increased both in TIFs of S100A4$^{+/+}$ tumors and in conditioned medium from S100A4-stimulated T lymphocytes (Fig. 6C).

Downloaded from http://aacrjournals.org/cancerres/article-pdf/70/3/936/2644381/936.pdf by guest on 13 April 2024

The result shown in Fig. 6D revealed that G-CSF was substantially increased in TIFs of 12-week-old mice compared with 6- or 18 ± 5-week-old mice.

Discussion

Our studies of spontaneous tumor development in MMTV-S100A4 GRS/A transgenic mice as well as clinical observations that correlate expression of S100A4 at early stages of breast cancer progression with poor prognosis (22, 27) led to the hypothesis that S100A4 modifies the tumor microenvironment at early stages of tumor development. We implemented the MMTV-PyMT mammary tumor model to analyze the role of S100A4 in premalignant tumor development by generating S100A4$^{-/-}$ PyMT mice. Tumor formation was not affected by S100A4 deficiency, but the resulting tumors had low vascular indices, which correlated with the suppression of pulmonary metastases. This has been shown in previous research on a similar tumor model on a BALB/c genetic background (28), indicating that the metastasis-inducing effect of S100A4 is independent of the genetic background.

Increased expression and release of S100A4 from tumor stroma cells was documented during the transition period from adenoma/MIN to early carcinoma. Furthermore, we

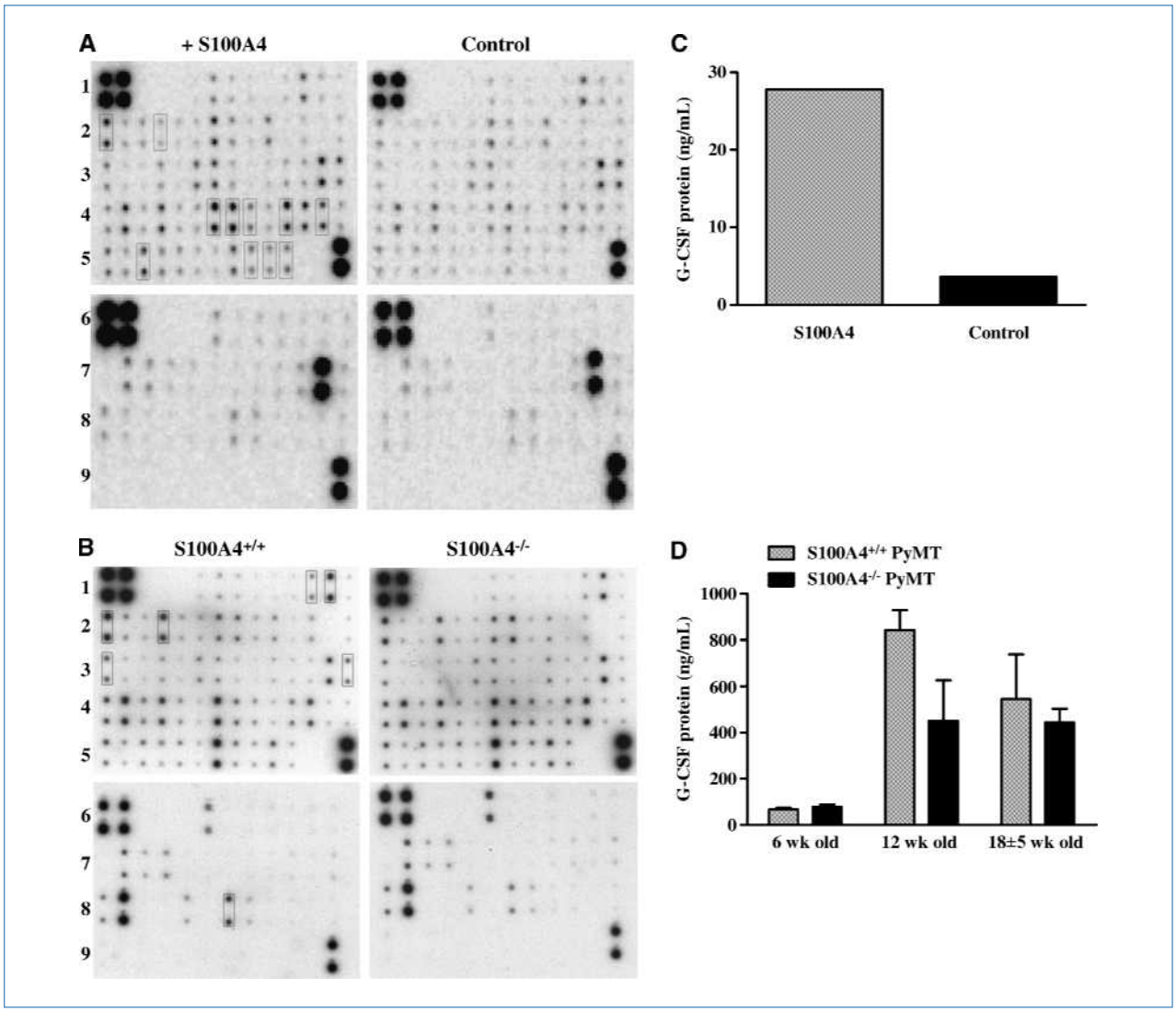

Figure 6. S100A4 stimulates production of cytokines from T lymphocytes. A, protein microarray analysis of conditioned medium from S100A4-activated T cells. Note that increased levels of the following 11 cytokines and growth factors are marked with rectangles (from left to right): row 2, eotaxin-2 and G-CSF; row 4, MIP-1γ, MIP-2, MIP-3β, PF-4, and RANTES; row 5, TCA-3, TPO, VCAM-1, and VEGF. B, protein microarray analysis of tumor TIFs from 12-wk-old S100A4$^{+/+}$ and S100A4$^{-/-}$ PyMT mice. Note that increased levels of the following seven cytokines in S100A4$^{+/+}$ TIFs compared with the S100A4$^{-/-}$ TIFs are marked with rectangles (from left to right): row 1, CTACK and CXCL16; row 2, eotaxin-2 and G-CSF; row 3, IL-4 and L-selectin; row 8, thymus CK-1. C, concentration of G-CSF in conditioned medium from T lymphocytes stimulated with S100A4. D, concentration of G-CSF protein in TIFs from S100A4$^{+/+}$ PyMT and S100A4$^{-/-}$ PyMT mice ages 6 (n = 5), 12 (n = 5), and 18 ± 5 (n = 4) wk.

Downloaded from http://aacrjournals.org/cancerres/article-pdf/70/3/936/2644381/936.pdf by guest on 13 April 2024

observed massive infiltration of macrophages and T cells at this transition period of tumor development, confirming earlier observations in the same mouse model (2). Macrophages and T cells are major components of the inflammatory cell population present in the tumor stroma. Particularly in breast cancer, these cells are regarded as causal players in primary cancer development and metastatic dissemination (3, 4, 29). It has been shown recently that the malignant transition of MMTV-PyMT–induced tumors is associated with the influx of macrophages (2). Comparing the amount of macrophages and T cells infiltrating adenoma/MIN in S100A4$^{+/+}$ and S100A4$^{-/-}$ tumors showed a decrease in both cell types in S100A4-deficient tumors. Although the reduction of the amount of macrophages was not statistically significant, the number of infiltrated T cells was substantially reduced. These observations suggested that an increase of S100A4 in the tumor microenvironment at premalignant stage contributed to the attraction of inflammatory cells to the developing tumor.

Generation of the protumor inflammatory microenvironment is mainly attributed to macrophages that facilitate the remodeling of the ECM, stimulation of angiogenesis, tumor cell migration, invasion, and eventually metastasis (4, 30). In the MMTV-PyMT mouse model, macrophages regulate the angiogenic switch and by this stimulate tumor progression (2).

The role of T cells in the generation of the protumor inflammatory microenvironment is much less understood. Earlier, the accumulation of T cells was considered as indicator of immune surveillance by the host. Simultaneously, numerous reports linked immune cell infiltration to poor prognosis (31). A study of the functional properties of tumor-infiltrating lymphocytes showed that they were largely inactive (31). Very recent data obtained by DeNardo and colleagues (6) convincingly showed that increased presence of CD4$^+$ T cells promotes metastasis of mammary carcinoma by enhancing the protumor activity of myeloid cells.

Here, we associated the S100A4-dependent suppression of the metastatic ability of MMTV-PyMT tumors with the lack of tumor-infiltrating T cells. *In vitro*, the S100A4 protein seemed to be a potent attractant of T cells. Moreover, T cells were attracted to tumor xenografts supplied with S100A4$^{+/+}$ MEFs as a source of S100A4 protein.

All this supports the presumption that S100A4 released into the microenvironment displays its activity at the transition to malignancy by attracting T cells to the early developing tumor. Dissemination of tumor cells occurs not only from the advanced tumors as it was considered earlier but also from the early epithelial alterations, such as hyperplasia and adenoma/MIN, in MMTV-PyMT mammary tumors (32). The events that facilitate the early spread could be associated with massive invasion of leukocytes that produce a plethora of molecules, which in turn modify the tumor microenvironment and stimulate angiogenesis.

T cells, activated by S100A4, produced cytokines and growth factors. Many of them are known as proinflammatory cytokines, which are associated with poor prognosis in cancer patients (33). Two cytokines were overproduced by S100A4-activated T cells and were present in increased amounts in TIFs of early S100A4$^{+/+}$ PyMT tumors. Enhanced G-CSF and eotaxin-2 were found both in TIFs isolated from early transition stage tumors of S100A4$^{+/+}$ mice and in conditioned medium from S100A4-activated T cells.

Eotaxin-2 (CCL24, MPIF-2), a proinflammatory cytokine, is a potent chemoattractant for eosinophils, which in some tumors (squamous cell carcinoma and colorectal tumors) was found to suppress the immune response and promote proliferation (34–36). G-CSF, another proinflammatory cytokine, is involved in the proliferation and differentiation of granulocytes and their precursors as well as in hematopoietic stem cell mobilization (37). G-CSF is routinely used during cancer chemotherapy to promote neutrophil proliferation and mobilization to decrease infections (38). Despite this, recent data pointed to the involvement of G-CSF in tumor progression and metastasis. G-CSF stimulated skin tumor progression and bone tumor growth (39–41). G-CSF production increased invasiveness of human head and neck carcinoma and hepatocarcinoma cell lines (42). Interestingly, G-CSF mediates mobilization of CD11b$^+$ Gr-1$^+$ myeloid cells that, as it was shown recently, stimulate metastatic spread of tumor (43, 44).

Attraction of T cells to the tumor xenografts supplied with MEFs as a source of S100A4 pointed to activated fibroblasts as a candidate cell type for the production of S100A4 and its release into the tumor microenvironment. Indeed, recent data obtained in our laboratory showed that tumor cells produced cytokines, such as RANTES, which stimulated secretion of S100A4 from fibroblasts.[3] Other cell types, including tumor cells, macrophages, mast cells, neutrophils, and certain classes of T cells, also could be stimulated to secrete S100A4 (11).

It has earlier been suggested that the accumulation of myeloid cells at the site of the primary tumor leads to the stimulation of the metastatic spread of tumor cells (1). Furthermore, myeloid cells also contributed to the formation of premetastatic niches by generating a favorable microenvironment for accepting tumor cells at sites in distant organs (3, 45, 46). Increased levels of extracellular S100A4 stimulated the accumulation of T cells at the site of the primary tumor; furthermore, S100A4$^{+/+}$ MEF-mediated accumulation of T cells occurred in premetastatic lungs. These observations allow us to speculate that S100A4 contributes to the generation of premetastatic niches. This could be achieved via attraction of T cells to the secondary site or indirectly via the stimulation of the production of cytokines (G-CSF) that will in turn attract myeloid cells to the site of future metastases.

CD4$^+$ T cells promote metastasis of mammary carcinoma by enhancing the protumor activity of myeloid cells (6). We can speculate that S100A4 mediates attraction and/or activation of these T cells to promote metastatic spread. It could also stimulate attraction of Gr-1$^+$ CD11b$^+$ myeloid precursors mediated by enhanced production of G-CSF (43).

Our data indicate that analogous process could occur in the site of secondary tumor development, where increased activity of S100A4 stimulates T-cell attraction, generates

[3] Forst et al., submitted for publication.

Downloaded from http://aacrjournals.org/cancerres/article-pdf/70/3/936/2644381/936.pdf by guest on 13 April 2024

inflammatory milieu, and thereby creates a favorable microenvironment to attract myeloid cells and generate a premetastatic niche. We propose therefore that lymphoid cells along with cells of myeloid lineage could be important components of the premetastatic niche.

Here, we provide strong evidence that the generation of an inflammatory milieu, including T cells and macrophages, in the tumor microenvironment stimulated metastatic spread of tumor cells.

Disclosure of Potential Conflicts of Interest

No potential conflicts of interest were disclosed.

Acknowledgments

We thank Birgitte Kaas, Hanne Nors, Ingrid Fosser-Larsen, and Lene Bregnholt Larsen for careful technical assistance.

Grant Support

European Union, FP7-Tumic, Health-F2-2008-201662, and Danish Cancer Society. B. Grum-Schwensen was supported by Danish Cancer Society, Dansk Kræftforsknings Fond, Familien Spogaards Fond, and Novo Nordisk Fonden.

The costs of publication of this article were defrayed in part by the payment of page charges. This article must therefore be hereby marked *advertisement* in accordance with 18 U.S.C. Section 1734 solely to indicate this fact.

Received 9/7/09; revised 12/1/09; accepted 12/3/09; published OnlineFirst 1/26/10.

References

1. DeNardo DG, Johansson M, Coussens LM. Immune cells as mediators of solid tumor metastasis. Cancer Metastasis Rev 2008;27:11–8.
2. Lin EY, Li JF, Gnatovskiy L, et al. Macrophages regulate the angiogenic switch in a mouse model of breast cancer. Cancer Res 2006;66:11238–46.
3. Kim S, Takahashi H, Lin WW, et al. Carcinoma-produced factors activate myeloid cells through TLR2 to stimulate metastasis. Nature 2009;457:102–6.
4. DeNardo DG, Coussens LM. Inflammation and breast cancer. Balancing immune response: crosstalk between adaptive and innate immune cells during breast cancer progression. Breast Cancer Res 2007;9:212.
5. Strauss L, Bergmann C, Szczepanski M, Gooding W, Johnson JT, Whiteside TL. A unique subset of $CD4^{+}CD25^{high}Foxp3^{+}$ T cells secreting interleukin-10 and transforming growth factor-β1 mediates suppression in the tumor microenvironment. Clin Cancer Res 2007;13:4345–54.
6. DeNardo DG, Barreto JB, Andreu P, et al. CD4(+) T cells regulate pulmonary metastasis of mammary carcinomas by enhancing protumor properties of macrophages. Cancer Cell 2009;16:91–102.
7. Guy CT, Cardiff RD, Muller WJ. Induction of mammary tumors by expression of polyomavirus middle T oncogene: a transgenic mouse model for metastatic disease. Mol Cell Biol 1992;12:954–61.
8. Lin EY, Jones JG, Li P, et al. Progression to malignancy in the polyoma middle T oncoprotein mouse breast cancer model provides a reliable model for human diseases. Am J Pathol 2003;163:2113–26.
9. Garrett SC, Varney KM, Weber DJ, Bresnick AR. S100A4, a mediator of metastasis. J Biol Chem 2006;281:677–80.
10. Yao R, Davidson DD, Lopez-Beltran A, Maclennan GT, Montironi R, Cheng L. The S100 proteins for screening and prognostic grading of bladder cancer. Histol Histopathol 2007;22:1025–32.
11. Cabezon T, Celis JE, Skibshoj I, et al. Expression of S100A4 by a variety of cell types present in the tumor microenvironment of human breast cancer. Int J Cancer 2007;121:1433–44.
12. Schmidt-Hansen B, Klingelhofer J, Grum-Schwensen B, et al. Functional significance of metastasis-inducing S100A4(Mts1) in tumor-stroma interplay. J Biol Chem 2004;279:24498–504.
13. Ambartsumian N, Klingelhofer J, Grigorian M, et al. The metastasis-associated Mts1(S100A4) protein could act as an angiogenic factor. Oncogene 2001;20:4685–95.
14. Novitskaya V, Grigorian M, Kriajevska M, et al. Oligomeric forms of the metastasis-related Mts1 (S100A4) protein stimulate neuronal differentiation in cultures of rat hippocampal neurons. J Biol Chem 2000;275:41278–86.
15. Belot N, Pochet R, Heizmann CW, Kiss R, Decaestecker C. Extracellular S100A4 stimulates the migration rate of astrocytic tumor cells by modifying the organization of their actin cytoskeleton. Biochim Biophys Acta 2002;1600:74–83.
16. Pedersen KB, Andersen K, Fodstad O, Maelandsmo GM. Sensitization of interferon-γ induced apoptosis in human osteosarcoma cells by extracellular S100A4. BMC Cancer 2004;4:52.
17. Schmidt-Hansen B, Ornas D, Grigorian M, et al. Extracellular S100A4 (mts1) stimulates invasive growth of mouse endothelial cells and modulates MMP-13 matrix metalloproteinase activity. Oncogene 2004;23:5487–95.
18. Boye K, Grotterod I, Aasheim HC, Hovig E, Maelandsmo GM. Activation of NF-κB by extracellular S100A4: analysis of signal transduction mechanisms and identification of target genes. Int J Cancer 2008;123:1301–10.
19. Klingelhofer J, Moller HD, Sumer EU, et al. Epidermal growth factor receptor ligands as new extracellular targets for the metastasis-promoting S100A4 protein. FEBS J 2009;276:5936–48.
20. Grum-Schwensen B, Klingelhofer J, Berg CH, et al. Suppression of tumor development and metastasis formation in mice lacking the S100A4(mts1) gene. Cancer Res 2005;65:3772–80.
21. Grigorian M, Ambartsumian N, Lukanidin E. Metastasis-inducing S100A4 protein: implication in non-malignant human pathologies. Curr Mol Med 2008;8:492–6.
22. Ambartsumian NS, Grigorian MS, Larsen IF, et al. Metastasis of mammary carcinomas in GRS/A hybrid mice transgenic for the mts1 gene. Oncogene 1996;13:1621–30.
23. Celis JE, Gromov P, Cabezon T, et al. Proteomic characterization of the interstitial fluid perfusing the breast tumor microenvironment: a novel resource for biomarker and therapeutic target discovery. Mol Cell Proteomics 2004;3:327–44.
24. Yanagawa Y, Iwabuchi K, Onoe K. Enhancement of stromal cell-derived factor-1α-induced chemotaxis for CD4/8 double-positive thymocytes by fibronectin and laminin in mice. Immunology 2001;104:43–9.
25. Stam JC, Michiels F, van der Kammen RA, Moolenaar WH, Collard JG. Invasion of T-lymphoma cells: cooperation between Rho family GTPases and lysophospholipid receptor signaling. EMBO J 1998;17:4066–74.
26. Baus E, Van LF, Andris F, Rolin S, Urbain J, Leo O. Dexamethasone increases intracellular cyclic AMP concentration in murine T lymphocyte cell lines. Steroids 2001;66:39–47.
27. Lee WY, Su WC, Lin PW, Guo HR, Chang TW, Chen HH. Expression of S100A4 and Met: potential predictors for metastasis and survival in early-stage breast cancer. Oncology 2004;66:429–38.
28. Xue C, Plieth D, Venkov C, Xu C, Neilson EG. The gatekeeper effect of epithelial-mesenchymal transition regulates the frequency of breast cancer metastasis. Cancer Res 2003;63:3386–94.
29. Ben-Baruch A. Host microenvironment in breast cancer development: inflammatory cells, cytokines and chemokines in breast cancer progression: reciprocal tumor-microenvironment interactions. Breast Cancer Res 2003;5:31–6.
30. Condeelis J, Pollard JW. Macrophages: obligate partners for tumor cell migration, invasion, and metastasis. Cell 2006;124:263–6.

Downloaded from http://aacrjournals.org/cancerres/article-pdf/70/3/936/2644381/936.pdf by guest on 13 April 2024

31. Whiteside TL. The tumor microenvironment and its role in promoting tumor growth. Oncogene 2008;27:5904–12.
32. Husemann Y, Geigl JB, Schubert F, et al. Systemic spread is an early step in breast cancer. Cancer Cell 2008;13:58–68.
33. Soria G, Ben-Baruch A. The inflammatory chemokines CCL2 and CCL5 in breast cancer. Cancer Lett 2008;267:271–85.
34. Lotfi R, Lee JJ, Lotze MT. Eosinophilic granulocytes and damage-associated molecular pattern molecules (DAMPs): role in the inflammatory response within tumors. J Immunother 2007;30:16–28.
35. Lampinen M, Carlson M, Hakansson LD, Venge P. Cytokine-regulated accumulation of eosinophils in inflammatory disease. Allergy 2004;59:793–805.
36. Cheadle EJ, Riyad K, Subar D, et al. Eotaxin-2 and colorectal cancer: a potential target for immune therapy. Clin Cancer Res 2007;13:5719–28.
37. Hunter MG, Jacob A, O'donnell LC, et al. Loss of SHIP and CIS recruitment to the granulocyte colony-stimulating factor receptor contribute to hyperproliferative responses in severe congenital neutropenia/acute myelogenous leukemia. J Immunol 2004;173:5036–45.
38. Smith TJ, Khatcheressian J, Lyman GH, et al. 2006 update of recommendations for the use of white blood cell growth factors: an evidence-based clinical practice guideline. J Clin Oncol 2006;24:3187–205.
39. Mueller MM. Inflammation in epithelial skin tumours: old stories and new ideas. Eur J Cancer 2006;42:735–44.
40. Obermueller E, Vosseler S, Fusenig NE, Mueller MM. Cooperative autocrine and paracrine functions of granulocyte colony-stimulating factor and granulocyte-macrophage colony-stimulating factor in the progression of skin carcinoma cells. Cancer Res 2004;64:7801–12.
41. Hirbe AC, Uluckan O, Morgan EA, et al. Granulocyte colony-stimulating factor enhances bone tumor growth in mice in an osteoclast-dependent manner. Blood 2007;109:3424–31.
42. Piscaglia AC, Shupe TD, Pani G, Tesori V, Gasbarrini A, Petersen BE. Establishment of cancer cell lines from rat hepatocholangiocarcinoma and assessment of the role of granulocyte-colony stimulating factor and hepatocyte growth factor in their growth, motility and survival. J Hepatol 2009;51:77–92.
43. Shojaei F, Wu X, Qu X, et al. G-CSF-initiated myeloid cell mobilization and angiogenesis mediate tumor refractoriness to anti-VEGF therapy in mouse models. Proc Natl Acad Sci U S A 2009;106:6742–7.
44. Yang L, Huang J, Ren X, et al. Abrogation of TGFβ signaling in mammary carcinomas recruits Gr-1^{+}CD11b^{+} myeloid cells that promote metastasis. Cancer Cell 2008;13:23–35.
45. Alison MR, Lim S, Houghton JM. Bone marrow-derived cells and epithelial tumours: more than just an inflammatory relationship. Curr Opin Oncol 2009;21:77–82.
46. Peinado H, Rafii S, Lyden D. Inflammation joins the “niche”. Cancer Cell 2008;14:347–9.

Downloaded from http://aacrjournals.org/cancerres/article-pdf/70/3/936/2644381/936.pdf by guest on 13 April 2024